Received: 5 June 2017 | Revised: 27 September 2017 | Accepted: 28 December 2017

DOI: 10.1002/jemt.22993

MRT LETTER

WILEY MICROSCOPY RESEARCH & TECHNIQUE

Two-frequency CARS imaging by switching fiber laser excitation

Eric C. Rentchler[1] | Ruxin Xie[2] | Rongqing Hui[2] | Carey K. Johnson[1]

[1]Department of Chemistry, University of Kansas, Lawrence, Kansas 66045

[2]Department of Electrical Engineering and Computer Science, University of Kansas, Lawrence, Kansas 66045

Correspondence
Carey K. Johnson, Department of Chemistry, University of Kansas, 1251 Wescoe Drive, Lawrence, Kansas 66045
Email: ckjohnson@ku.edu

Funding information
National Institutes of Health, Grant/Award Number: R21GM103478

Review Editor: Dr. Paolo Bianchini

Abstract

To fully exploit the power of coherent Raman imaging, techniques are needed to image more than one vibrational frequency simultaneously. We describe a method for switching between two vibrational frequencies based on a single fiber-laser source. Stokes pulses were generated by soliton self-frequency shifting in a photonic crystal fiber. Pump and Stokes pulses were stretched to enhance vibrational resolution by spectral focusing. Stokes pulses were switched between two wavelengths on the millisecond time scale by a liquid-crystal retarder. Proof-of-principle is demonstrated by coherent anti-Stokes Raman imaging of polystyrene beads embedded in a poly(methyl methacrylate) (PMMA) matrix. The Stokes shift was switched between 3,050 cm^{-1}, where polystyrene has a Raman transition, and 2,950 cm^{-1}, where both polystyrene and PMMA have Raman resonances. The method can be extended to multiple vibrational modes.

KEYWORDS
CARS imaging, fiber laser, multiplexing, photonic crystal fiber

1 | INTRODUCTION

Microscopy based on coherent Raman scattering couples label-free imaging of molecular vibrational modes with the benefits of multiphoton spectroscopy—optical sectioning and the penetration depth of near-infrared excitation (Camp & Cicerone, 2015; Cheng & Xie, 2015; Zumbusch, Holtom, & Xie, 1999). However, applications of coherent Raman imaging have been limited by the need for expensive or complex excitation sources to supply the pump and Stokes beams. In our laboratory we developed a fiber laser excitation (FLEx) source for coherent Raman imaging based on a single fiber laser and a photonic crystal fiber (PCF) (Adany, Arnett, Johnson, & Hui, 2011; Su, Xie, Johnson, & Hui, 2013; Xie et al., 2014). Our goal is the development of a robust, compact, and relatively inexpensive source for coherent Raman imaging.

Various methods have been used to generate pump and Stokes beams from a single laser source (Camp & Cicerone, 2015). Several labs have demonstrated coherent Raman imaging in which either the pump or the Stokes beam is generated in a PCF (Adany et al., 2011; Andresen, Birkedal, Thøgersen, & Keiding, 2006; Andresen, Nielsen, Thøgersen, & Keiding, 2007; Andresen, Paulsen, Birkedal, Thøgersen, & Keiding, 2005; Paulsen, Hilligse, Thøgersen, Keiding, & Larsen, 2003; Pegoraro et al., 2009; Zhai et al., 2011). In some implementations, the PCF is used to generate a super-continuum, allowing tuning by changing the time delay between pump and Stokes beams. We and others used soliton self-frequency shifting in a PCF to generate a nearly bandwidth-limited Stokes beam (Adany et al., 2011; Andresen et al., 2006, 2007; Su et al., 2013). As the extent of soliton self-frequency shifting depends on the optical power coupled into the PCF (Agrawal, 2001), modulation of the optical power coupled into the PCF allows tuning of the soliton wavelength, opening the possibility to probe multiple Raman resonances.

Promising approaches for multiplex coherent anti-Stokes Raman (CARS) have been developed in which multiple vibrational modes can be probed simultaneously (Alshaykh et al., 2017; Burkacky, Zumbusch, Brackmann, & Enejder, 2006; Camp & Cicerone, 2015; Cheng, Volkmer, Book, & Xie, 2002; Cicerone & Kee, 2004; Liao et al., 2016; Müller & Schins, 2002). These methods are typically based on broad-band (or multiple) pump or Stokes pulses combined with a narrow bandwidth beam (Stokes or pump) to permit collection of the CARS spectrum at any point in the image by analysis of the CARS signal in a spectral analyzer or spectrograph. Rapid frequency-modulation CARS (FM-CARS) has also been demonstrated previously, where it has been used to remove nonresonant background from CARS signals (Chen, Sung, & Lim, 2010; Ganikhanov, Evans, Saar, & Xie, 2006; Saar et al., 2009).

In this article, we describe dual-frequency CARS by switching the Stokes wavelength in the PCF. Dual-frequency excitation by PCF switching was previously implemented in our lab for two-photon

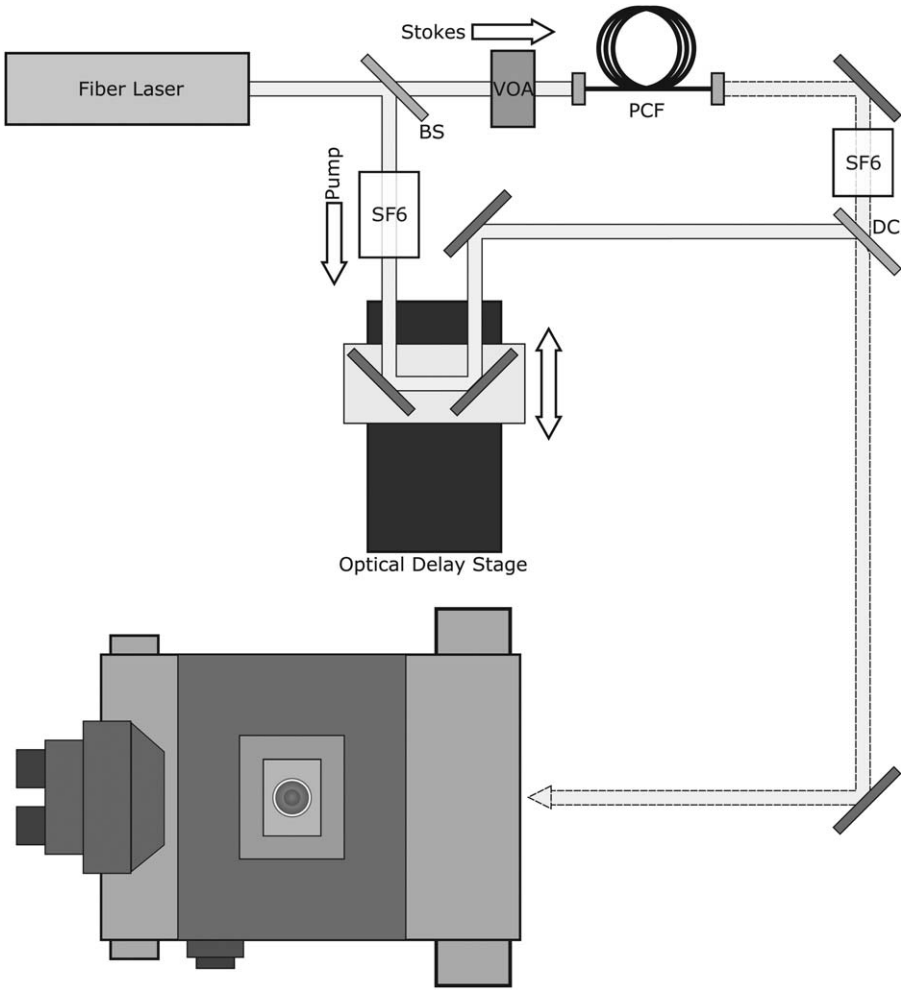

FIGURE 1 Schematic of the optical setup. The beam from the fiber laser at 802 nm was split in the beam splitter (BS). In the Stokes channel, the wavelength of the soliton generated in the photonic crystal fiber (PCF) was controlled by modulating the beam power with a variable optical attenuator (VOA). Stokes pulses were chirped in SF6 glass. The pump pulses were also stretched in SF6 glass and delayed to overlap Stokes pulses. Pump and Stokes beams were recombined by a dichroic beam splitter (DC), and the combined beams were directed into the microscope

imaging (Adany, Johnson, & Hui, 2012; Unruh et al., 2006). We also demonstrated switching of the soliton wavelength in 5 μs by modulating the optical power with a ceramic electro-optic modulator (Adany, Price, Johnson, Zhang, & Hui, 2009). In coherent Raman imaging, fast switching between vibrational modes at each pixel offers the possibility to simultaneously generate two distinct CARS images probing different vibrational frequencies.

The method we describe here has the virtues of simplicity and speed. Pump and Stokes beams are derived from the same fiber laser. Rapid switching between two or more Stokes wavelengths on the millisecond time scale allows simultaneous acquisition of CARS images for two or more vibrational modes. Multiple Raman shifts (two in the work presented here) can be probed rapidly, pixel-by-pixel, with a single FLEx source and without a spectral analyzer (Adany et al., 2009). In this report we demonstrate switching CARS imaging with a sample of polystyrene beads imbedded in a matrix of poly(methyl methacrylate)(PMMA). Rapid Stokes switching allows simultaneous imaging of C-H stretching modes of polystyrene and the PMMA matrix. The method can be extended in principle to multiple Raman bands.

2 | METHODS

For proof-of-principle we used a sample consisting of 15 μm polystyrene microspheres embedded in a PMMA matrix. The sample was prepared by mixing the polystyrene microspheres with 8-μm PMMA microspheres at a 1:4 ratio of polystyrene to PMMA. The microsphere mixture was placed on a coverslip and heated to a temperature at which the PMMA microspheres melted while the polystyrene microspheres remained intact. Prior to the sample cooling, a coverslip was placed onto the top of the sample cell. The sample thickness was ~200 μm.

The CARS imaging system is depicted schematically in Figure 1. Pump pulses were generated by a fiber laser generating 100-fs pulses with a 75-MHz repetition rate at 802 nm (Femtolite-100, IMRA

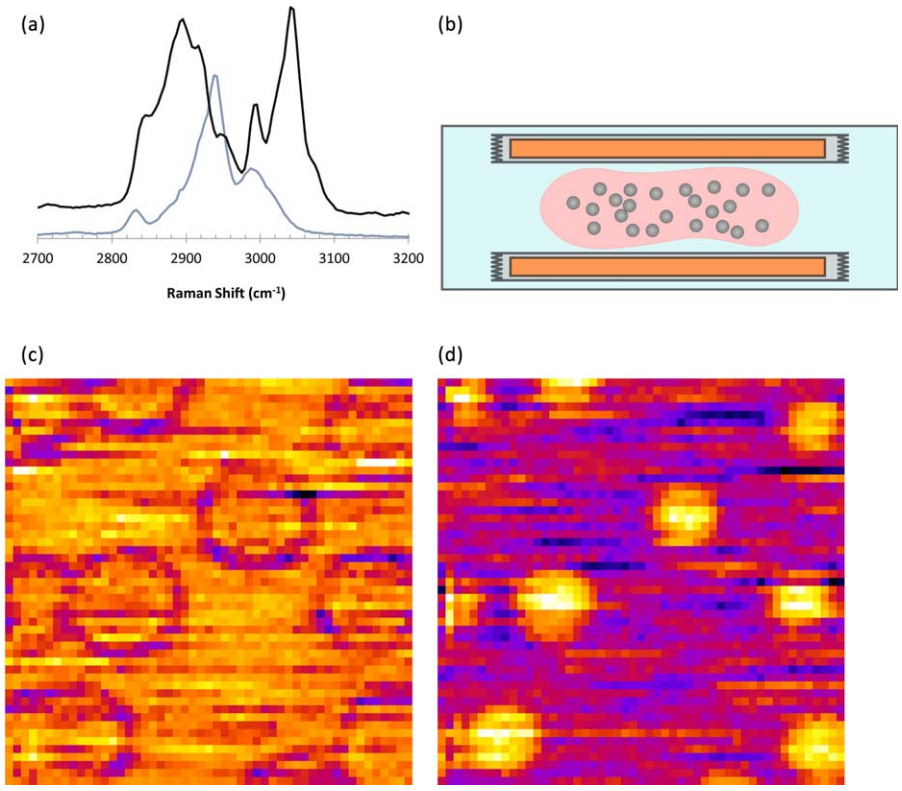

FIGURE 2 (a) The Raman spectra of PMMA (blue) and polystyrene (black). (b) Schematic of polystyrene beads (gray) embedded in PMMA (pink). (c) and (d) show 50 × 50 μm images of 15 μm polystyrene beads embedded in PMMA. Images were collected probing at 2,950 cm^{-1} (c) and at 3,050 cm^{-1} (d). In (c) the signal is generated from both the polystyrene microspheres and the PMMA background, whereas in (d) at 3,050 cm^{-1} the signal is dominated by the polystyrene resonance [Color figure can be viewed at wileyonlinelibrary.com]

America, Inc., Ann Arbor, MI). The beam was split with a 50% beam splitter, and one portion of the beam was focused into a 2-m long PCF (NL-1.8–710, Thorlabs Inc., Newton, NJ). Pulses focused into the PCF shift to longer wavelengths by soliton self-frequency shifting (Nishizawa & Goto, 2001). The peak wavelength increases with increasing optical power coupled into the fiber (Gordon, 1986). Hence, the wavelength of the Stokes beam can be tuned by modulating the power coupled into the fiber. Spectra of Stokes pulses shifted by soliton self-frequency shifting have been published previously (Su et al., 2013). The optical power incident on the PCF was controlled by a liquid crystal variable retarder (LCC1221-B, Thorlabs). The retardation in the liquid crystal has rise and fall times of 14 ms and 510 μs, respectively, in response to a change in the applied voltage. The retarded beam was passed through a linear polarizer whose transmission axis matched the polarization incident on the liquid crystal retarder. Modulation of the beam polarization thus resulted in modulation of the optical power transmitted by the polarizer and coupled into the PCF. This allows switching between two Stokes frequencies in under 20 ms.

Both pump and Stokes beams were chirped in SF6 glass to enhance vibrational resolution by spectral focusing (Bartels, Weinacht, Leone, Kapteyn, & Murnane, 2002; Gershgoren et al., 2003; Hellerer, Enejder, & Zumbusch, 2004; Rocha-Mendoza, Langbein, & Borri, 2008). Pump and Stokes beams were focused into the sample with a 100× objective lens (Nikon CFI Superfluor 100x/1.3 NA). Pump and Stokes beam powers at the sample were 9 mW and 0.2 mW, respectively. The CARS signal was collected in the forward direction by a 40× objective lens (Olympus LCPLanFI 40x/0.6 NA) and detected by an Ocean Optics spectrometer (Maya 2000 pro). A piezoelectric scanning stage (Nano-H100-X-Nano-H100-Y, Mad City Labs) was used to raster-scan the sample across the focal point of the microscope. For switching CARS images, signals at each pixel were collected at both Stokes frequencies with a dwell time of about 120 ms before moving the piezoelectric stage for the next pixel. Data collection, sample scanning, and switching between Stokes frequencies were controlled by a MATLAB program. The control voltage applied to the liquid crystal was adjusted by a feedback loop to stabilize the frequency of the Stokes beam.

3 | RESULTS AND DISCUSSION

The possibility for fast switching of the Stokes wavelength is a consequence of generation of the Stokes beam by soliton self-frequency shifting in the PCF. When ultrafast pulses with high peak power are focused into the PCF, a soliton is established at a wavelength where anomalous dispersion in the PCF balances the effect of Kerr nonlinearity (Lee, Howe, Xu, & Liu, 2008). The fundamental soliton shifts to longer wavelength with increasing optical power due to the increase of chromatic dispersion in the fiber with wavelength. Rapid modulation of the power coupled into the fiber thus translates into rapid wavelength switching.

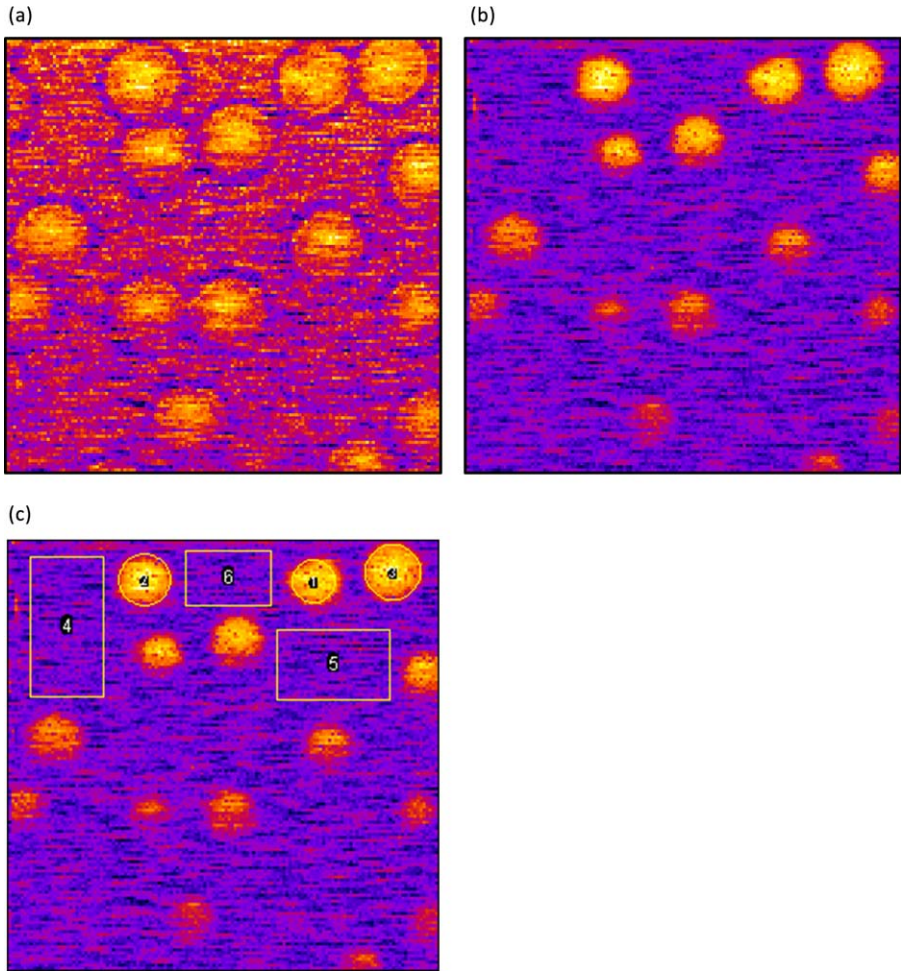

FIGURE 3 Fast-switching imaging of 15 μm polystyrene beads embedded in PMMA. The Stokes beam was switched between 1,050 nm (a) and 1,060 nm (b). The images are 70 × 70 μm. C shows the regions selected for comparison between the two images. The ratios between the average signals generated in polystyrene beads (regions 1–3) and the averages signals generated in the PMMA matrix (regions 4–6) are 1.5 in the 1,050-nm image and 3.1 in the 1,060-nm image [Color figure can be viewed at wileyonlinelibrary.com]

Rapid switching opens up the possibility to collect two or more CARS images simultaneously by switching the Stokes frequency between two vibrational modes of interest at each pixel. With sufficient spectral resolution, the system can selectively image populations within the sample that have different vibrational signatures (Adany et al., 2009; Su et al., 2013). Spectral resolution is achieved by spectral focusing, in which both pump and Stokes pulses are chirped linearly so that the frequency difference $\Delta\nu$ between the two beams remains (approximately) constant over the duration of the pulses (Bartels et al., 2002; Gershgoren et al., 2003; Hellerer et al., 2004; Rocha-Mendoza et al., 2008; Su et al., 2013). The frequency difference was matched to the desired vibrational resonance by tuning the soliton self-frequency shift in the PCF. Switching of the Stokes beam frequency thus allows switching between different vibrational resonances.

A model system consisting of PMMA and polystyrene microspheres was imaged to demonstrate the switching imaging abilities of the FLEx-CARS microscope. These materials were selected because their Raman spectra are similar but not identical, allowing selective imaging of each material. The Raman spectra of PMMA and polystyrene plotted together are shown in Figure 2a. PMMA has C-H stretching vibrational bands in the region from 2,824 cm^{-1} to 3,030 cm^{-1}, while polystyrene's C-H stretches appear in the region from 2,824 cm^{-1} to 3,083 cm^{-1}. Because of the high overlap between the vibrational spectra of the two polymers from 2,824 cm^{-1} to 3,030 cm^{-1}, it is possible to image both polystyrene and PMMA microspheres simultaneously.

Figure 2b shows a schematic of the sample. Images of the 15-μm polystyrene microspheres immobilized in a PMMA matrix were first collected sequentially, without switching, at two different Stokes shifts, Figure 2c,d. Because of chromatic dispersion in the PCF, SF6 glass, and other optical elements, temporal overlap between the pump and Stokes pulses was slightly altered upon shifting the wavelength of the Stokes beam (Su et al., 2013). Chirping of the pump and Stokes beams relaxes the need for optimum overlap. For the images in Figure 2c,d the delay line position was adjusted for each image to optimize temporal overlap between the chirped pump and Stokes pulses. The image collected at a Stokes shift of 2,950 cm^{-1} has a strong signal from both the 15-μm polystyrene microspheres as well as the PMMA matrix. This is to be expected as 2,950 cm^{-1} is in the region where the Raman spectra of PMMA and polystyrene overlap strongly. The second image was

collected with a Stokes shift of 3,050 cm^{-1}. In this image, only polystyrene beads contribute to the signal, but not PMMA.

For imaging with Stokes switching at each pixel, the delay line was set to the average of the optimum delays for vibrational frequencies of 2,950 cm^{-1} and 3,050 cm^{-1}. As a result of having chosen a time delay between the optimum delays for 2,950 cm^{-1} and 3,050 cm^{-1} individually, the temporal overlap of pump and Stokes pulses was not quite optimal for either vibrational band. The peak Stokes wavelengths were therefore adjusted to optimize the signals at 2,950 cm^{-1} and 3,050 cm^{-1}. It was found that at the set delay, the optimal peak Stokes wavelengths were 1,050 nm and 1,060 nm. As expected, the optimum Stokes wavelengths were closer together for the compromise setting of the delay line than the optimum delay settings for the two bands taken individually (Su et al., 2013). Switching images with Stokes beam switching at each pixel were then collected with the new combination of Stokes frequencies and delay. The resulting 70 × 70 μm images are shown in Figure 3. In image 3A a strong anti-Stokes signal is generated from both the PMMA and polystyrene microspheres, while in image 3B the signal is mostly produced by the polystyrene microspheres.

A quantitative analysis was performed for six areas within the images. The signals from three regions centered on polystyrene beads and three in the PMMA matrix were compared in the two images. The regions selected are shown in Figure 3c. In the image collected with a 1,050-nm Stokes beam the ratio of the signal from polystyrene regions to the signal from PMMA sum was 1.5, while in the image collected at 1,060 nm the ratio of the polystyrene sum to the PMMA sum increased to 3.1. This increase was expected, because there should be a much stronger anti-Stokes signal generated at 3,066 cm^{-1} by polystyrene. The results confirm the contrast between images collected at two different Stokes wavelengths.

In the current implementation of the FLEx-CARS system, image quality is limited by the Stokes beam power, which is in turn limited by the power of the fundamental soliton carried by the first-order mode of the PCF. For future implementations of FLEx-CARS imaging the Stokes beam power could be increased by utilizing a higher-order mode in a PCF exhibiting anomalous dispersion. This would effectively increase the mode field diameter in the fiber core, allowing a higher power of the Stokes beam to satisfy the fundamental soliton condition (Lee et al., 2008). Image quality could also be improved by frequency modulation to discriminate against nonresonant background. Further enhancement of image quality could be achieved by more rapid switching, for example by using a faster Pockels cell (e.g., KD*P) or with a ceramic electro-optic modulator (Adany et al., 2009), instead of a liquid crystal retarder. Galvanometric scanning would allow a much faster acquistion speed, which would allow for image averaging and smaller step sizes to produce crisper images.

4 | CONCLUSIONS

We have demonstrated the ability to selectively and simultaneously generate two CARS images from a model sample. Fast switching imaging is inherent to the FLEx-CARS microscope design. The Stokes wavelength was controlled with a liquid-crystal retarder, which modulated the power focused into the PCF. Other devices offer even faster switching times. Both the number of multiplexed frequencies and the switching speed can thus be increased in future iterations of the FLEx-CARS microscope.

ACKNOWLEDGMENTS

The authors thank Prof. Judy Wu and her research group for use of the Raman microscope and assistance in acquisition of the spontaneous Raman spectrum of PMMA and polystyrene. This work was supported by grant number R21GM103478 from the National Institutes of Health.

ORCID

Carey K. Johnson http://orcid.org/0000-0002-4207-8039

REFERENCES

Adany, P., Arnett, D. C., Johnson, C. K., & Hui, R. (2011). Tunable excitation source for coherent Raman spectroscopy based on a single fiber laser. *Applied Physics Letters*, *99*, 181112–1811123.

Adany, P., Johnson, C. K., & Hui, R. (2012). Fiber laser based two-photon FRET measurement of calmodulin and mCherry-E(0) GFP proteins. *Microscopy Research and Technique*, *75*, 837–843.

Adany, P., Price, E. S., Johnson, C. K., Zhang, R., & Hui, R. (2009). Switching of 800 nm femtosecond laser pulses using a compact PMN-PT modulator. *The Review of Scientific Instruments*, *80*, 033107.

Agrawal, G. P. (2001). *Nonlinear fiber optics*. San Diego, CA: Academic.

Alshaykh, M. S., Liao, C.-S., Sandoval, O. E., Gitzinger, G., Forget, N., Leaird, D. E., … Weiner, A. M. (2017). High-speed stimulated hyperspectral Raman imaging using rapid acousto-optic delay lines. *Optics Letters*, *42*, 1548–1551.

Andresen, E. R., Birkedal, V., Thøgersen, J., & Keiding, S. R. (2006). Tunable light source for coherent anti-Stokes Raman scattering microspectroscopy based on the soliton self-frequency shift. *Optics Letters*, *31*, 1328–1330.

Andresen, E. R., Nielsen, C. K., Thøgersen, J., & Keiding, S. R. (2007). Fiber laser-based light source for coherent anti-Stokes Raman scattering microspectroscopy. *Optics Express*, *15*, 4848–4856.

Andresen, E. R., Paulsen, H. N., Birkedal, V., Thøgersen, J., & Keiding, S. R. (2005). Broadband multiplex coherent anti-Stokes Raman scattering microscopy employing photonic-crystal fibers. *Journal of the Optical Society of America B*, *22*, 1934–1938.

Bartels, R. A., Weinacht, T. C., Leone, S. R., Kapteyn, H. C., & Murnane, M. M. (2002). Nonresonant control of multimode molecular wave packets at room temperature. *Physical Review Letters*, *88*, 033001.

Burkacky, O., Zumbusch, A., Brackmann, C., & Enejder, A. (2006). Dual-pump coherent anti-Stokes-Raman scattering microscopy. *Optics Letters*, *31*, 3656–3658.

Camp, C. H., Jr., & Cicerone, M. T. (2015). Chemically sensitive bioimaging with coherent Raman scattering. *Nature Photonics*, *9*, 295–305.

Chen, B.-C., Sung, J., & Lim, S.-H. (2010). Chemical imaging with frequency modulation coherent anti-Stokes Raman scattering microscopy at the vibrational fingerprint region. *The Journal of Physical Chemistry B*, *114*, 16871–16880.

Cheng, J.-X., Volkmer, A., Book, L. D., & Xie, X. S. (2002). Multiplex coherent anti-Stokes Raman scattering microspectroscopy and study of lipid vesicles. *The Journal of Physical Chemistry B*, *106*, 8493–8498.

Cheng, J.-X., & Xie, X. S. (2015). Vibrational spectroscopic imaging of living systems: An emerging platform for biology and medicine. *Science*, *350*, 1054.

Cicerone, M. T., & Kee, T. W. (2004). Broadband CARS microscopy. *Microscopy Today*, *12*, 38–40.

Ganikhanov, F., Evans, C. L., Saar, B. G., & Xie, X. S. (2006). High-sensitivity vibrational imaging with frequency modulation coherent anti-Stokes Raman scattering (FM CARS) microscopy. *Optics Letters*, *31*, 1872–1874.

Gershgoren, E., Bartels, R. A., Fourkas, J. T., Tobey, R., Murnane, M. M., & Kapteyn, H. C. (2003). Simplified setup for high-resolution spectroscopy that uses ultrashort pulses. *Optics Letters*, *28*, 361–363.

Gordon, J. P. (1986). Theory of the soliton self-frequency shift. *Optics Letters*, *11*, 662–664.

Hellerer, T., Enejder, A. M. K., & Zumbusch, A. (2004). Spectral focusing: High spectral resolution spectroscopy with broad-bandwidth laser pulses. *Applied Physics Letters*, *85*, 25–27.

Lee, J. H., Howe, J., Xu, C., & Liu, X. (2008). Soliton self-frequency shift: experimental demonstrations and applications. *IEEE Journal of Selected Topics in Quantum Electronics*, *14*, 713–723.

Liao, C.-S., Huang, K.-C., Hong, W., Chen, A. J., Karanja, C., Wang, P., … Cheng, J.-X. (2016). Stimulated Raman spectroscopic imaging by microsecond delay-line tuning. *Optica*, *3*, 1377–1380.

Müller, M., & Schins, J. M. (2002). Imaging the thermodynamic state of lipid membranes with multiplex CARS microscopy. *The Journal of Physical Chemistry B*, *106*, 3715–3723.

Nishizawa, N., & Goto, T. (2001). Widely wavelength-tunable ultrashort pulse generation using polarization maintaining optical fibers. *IEEE Journal of Selected Topics in Quantum Electronics*, *7*, 518–524.

Paulsen, H. N., Hilligse, K. M., Thøgersen, J., Keiding, S. R., & Larsen, J. J. (2003). Coherent anti-Stokes Raman scattering microscopy with a photonic crystal fiber based light source. *Optics Letters*, *28*, 1123–1125.

Pegoraro, A. F., Ridsdale, A., Moffatt, D. J., Jia, Y., Pezacki, J. P., & Stolow, A. (2009). Optimally chirped multimodal CARS microscopy based on a single Ti:sapphire oscillator. *Optics Express*, *17*, 2984–2996.

Rocha-Mendoza, I., Langbein, W., & Borri, P. (2008). Coherent anti-Stokes Raman microspectroscopy using spectral focusing with glass dispersion. *Applied Physics Letters*, *93*, 201103/1–201103/3.

Saar, B. G., Holtom, G. R., Freudiger, C. W., Ackermann, C., Hill, W., & Xie, X. S. (2009). Intracavity wavelength modulation of an optical parametric oscillator for coherent Raman microscopy. *Optics Express*, *17*, 12532–12539.

Su, J., Xie, R., Johnson, C. K., & Hui, R. (2013). Single fiber laser based wavelength tunable excitation for CRS spectroscopy. *Journal of the Optical Society of America. B, Optical Physics*, *30*, 1671–1682.

Unruh, J. R., Price, E. S., Molla, R. G., Stehno-Bittel, L., Johnson, C. K., & Hui, R. (2006). Two-photon microscopy with wavelength switchable fiber laser excitation. *Optics Express*, *14*, 9825–9831.

Xie, R., Su, J., Hui, R., Rentchler, E. C., Johnson, C. K., Zhang, Z., & Shi, H. (2014). Multi-modal label-free imaging based on a femtosecond fiber laser. *Biomedical Optics Express*, *5*, 2390–2396.

Zhai, Y.-H., Goulart, C., Sharping, J. E., Wei, H., Chen, S., Tong, W., … Cheng, J.-X. (2011). Multimodal coherent anti-Stokes Raman spectroscopic imaging with a fiber optical parametric oscillator. *Applied Physics Letters*, *98*, 191106/1–191106/3.

Zumbusch, A., Holtom, G. R., & Xie, X. S. (1999). Three-dimensional vibrational imaging by coherent anti-Stokes Raman scattering. *Physical Review Letters*, *82*, 4142–4145.

How to cite this article: Rentchler EC, Xie R, Hui R, Johnson CK. Two-frequency CARS imaging by switching fiber laser excitation. *Microsc Res Tech*. 2018;81:413–418. https://doi.org/10.1002/jemt.22993